ICES Journal of Marine Science

ICES CIEM International Council for the Exploration of the Sea / Conseil International pour l'Exploration de la Mer

ICES Journal of Marine Science (2020), 77(2), 655–667. doi:10.1093/icesjms/fsz239

Original Article

Integration of bioenergetics in an individual-based model to hindcast anchovy dynamics in the Bay of Biscay

Juan Bueno-Pardo [1]*, Pierre Petitgas[2], Susan Kay[3], and Martin Huret [1]

[1]Ifremer, STH/LBH, BP 70, 29280 Plouzané, France
[2]Ifremer, EMH, Rue de l'Ile d'Yeu, BP 21105, 44311 Nantes Cedex 3, France
[3]Plymouth Marine Laboratory, Prospect Place, The Hoe, Plymouth PL1 3DH, UK

*Corresponding author: tel: +34 607 612 373; e-mail: jbuenopardo@gmail.com.

Bueno-Pardo, J., Petitgas, P., Kay, S., and Huret, M. Integration of bioenergetics in an individual-based model to hindcast anchovy dynamics in the Bay of Biscay. – ICES Journal of Marine Science, 77: 655–667.

Received 23 May 2019; revised 19 October 2019; accepted 15 November 2019; advance access publication 10 December 2019.

The population of European anchovy of the Bay of Biscay collapsed at the beginning of the 21st century, causing the closure of its fishery between 2005 and 2010. In order to study both the human and environmental causes of the anchovy population dynamics, an approach coupling individual bioenergetics to an individual-based model was applied between 2000 and 2015. This modelling framework was forced with outputs from a physical–biogeochemical model. In addition to a base-case scenario with realistic forcing, alternative scenarios were run without inter-annual variability in either fishing mortality or environmental conditions. During the decrease in population biomass, a high fishing pressure coincided with a combination of environmental variables promoting the appearance of large individuals that could not survive severe winters because of their high energetic demands. The recovery of the population was favoured by a period of warm years with abundant food favouring the winter survival of age 1 individuals, in coincidence with the closure of the fishery. Our modelling approach also allows to test the consequences of a retrospective implementation of the current harvest control rule from 2000 which, according to our results, would have prevented the collapse of the population and avoided the fishery closure.

Keywords: anchovy, Bay of Biscay, Dynamic Energy Budget, fishery, harvest control rule, individual-based model, population collapse.

Introduction

Like other small pelagic fish with a short lifespan, early maturation and high reproductive potential, the European anchovy (*Engraulis encrasicolus*) plays a pivotal ecological role due to its intermediate trophic position, high abundance, and energy content (Cury *et al.*, 2000; Palomera *et al.*, 2007). The population dynamics of small pelagic fish are often abrupt and tightly tied to environmental features by complex relationships (Checkley *et al.*, 2009). Environmental forcing is known to affect population dynamics through both biological (e.g. changes in life-history traits, physiological optima, behaviour, etc.) and physical (e.g. affecting survival, larval dispersion, feeding, etc.) pathways (Checkley *et al.*, 2009).

In the Bay of Biscay (NE Atlantic), the anchovy population sustains a valuable fishery shared by France and Spain. The historical evolution of landings of anchovy peaked between 1960 and 1965, with ca. 75 000 tonnes per year, while minimal landings occurred at the beginning of the 21st century (ICES, 2018). In 2005, the population reached a historical minimum that forced the closure of the fishery between 2005 and 2010, entailing important socio-economic consequences (Vermard *et al.*, 2008). The effect of fishing and environmental variables has been widely studied to understand both the drivers of this population and the causes of its collapse and, although a wide variety of approaches have been applied in this regard, few have succeeded in understanding the underlying biological or ecological mechanisms.

The literature on the effects of fishing and environment on the populations of small pelagic fish typically considers two levels of biological organization: populations and individuals (physiology). Among the first group, time-series correlation analyses have been used with different results. Hence, while the anchovy recruitment was not found to be related to zooplankton concentration (Irigoien *et al.*, 2009), the East-Atlantic oscillation index successfully explained part of the recruitment failure at the beginning of the 21st century (Borja *et al.*, 2008). Similarly, recruitment was found to be positively and negatively correlated to the magnitude of coastal upwelling and the degree of shelf stratification, respectively (Allain *et al.*, 2001). Other studies found that larval survival was related to anchovy spawning distribution (Allain *et al.*, 2007). Using a Bayesian approach, Taboada and Anadón (2016) showed that changes in phytoplankton phenology and larval drift presented good prediction indicators for the dynamics of the population but, to explain the collapse of the population, fishing pressure needed to be considered, improving considerably the skill of the models. At the individual/physiological level, several studies tried to determine the effect of environmental variables on life-history traits such as growth (Cotano *et al.*, 2008), mortality rates (Cotano *et al.*, 2008; Uriarte *et al.*, 2016), or reproduction (Motos, 1996; Somarakis *et al.*, 2004). As far as we know, none of the previous works developed a mechanistic approach linking the effect of environmental conditions to the response of the population based on the physiology of individuals.

The Dynamic Energy Budget (DEB) theory (Kooijman, 2010) is a metabolic-ecology theory describing the acquisition, use, and distribution of energy by individuals through metabolic reactions. In DEB theory, the energy from the environment is allocated through assimilation into three different compartments as follows: structure, maintenance, and reproduction/maturation, while temperature controls the velocity of all the metabolic reactions and fluxes of energy within the organism. Hence, the DEB theory facilitates understanding of the relationships between an individual's energy and life-history traits such as growth, reproduction, and mortality rates. A model based on the DEB theory has recently been assembled for the anchovy in the Bay of Biscay, describing its bioenergetics at annual and life-cycle scales (Gatti *et al.*, 2018). These kind of bioenergetic approaches are also useful to compare the life histories of individuals among geographic regions (Huret *et al.*, 2019), and for understanding the variations in vital rates found in response to environmental fluctuations (Pethybridge *et al.*, 2013; Politikos *et al.*, 2015a, b). Integrating the information from different individuals, DEB models can further be scaled up to the population level using individual-based models (IBMs, see Huse *et al.*, 2002). The use of IBMs to infer the consequences of environmental changes on small pelagic fish populations has grown since the 1990s (e.g. Letcher *et al.*, 1996; Rose *et al.*, 1999), but it was only after the inclusion of the full life cycle of fish (e.g. Jakobsen *et al.*, 2009) that IBMs succeeded in capturing the effect of environmental variables on aspects such as reproduction and mortality (e.g. Fietcher *et al.*, 2015; Politikos *et al.*, 2018). In the case of anchovy, a plankton feeder, models considering low trophic levels (physical–biogeochemical models) provide the energy from the environment in the form of food (plankton) and temperature. In this manner, life-history traits such as growth, reproduction, mortality, or movement can be related to the environmental variables and, integrating these phenomena over an entire population, the response of the population can be simulated (Pethybridge *et al.*, 2013; Politikos *et al.*, 2015b).

In this work, we integrate the bioenergetics of individual anchovies, using a DEB model forced with the outputs of a coupled physical–biogeochemical model, into a population (IBM) model, in order to create a unique mechanistic framework enabling us to understand the causes of the rapid collapse and slow recovery of the population between 2000 and 2015. This approach goes a step beyond the historical complexity of models for anchovy in the Bay of Biscay and is used to study the human and environmental effects on anchovy dynamics, by simulating different scenarios of environmental and fishing pressures. Finally, the implementation of the current harvest control rule (HCR) from the beginning of the century is simulated, in order to test whether this measure could have prevented the collapse of the population between 2005 and 2010.

Material and methods

In order to scale-up the effect of environmental variables on the anchovy's bioenergetics and evaluate the response at the population level, a joint modelling framework consisting of a DEB model and an IBM was assembled (Figure 1). This approach used the outputs (temperature and zooplankton concentration) from a regional physical–biogeochemical model as forcing for the DEB model for the anchovy described in Gatti *et al.* (2017). Then, an IBM integrated the response of the different individuals considered within the population (in terms of growth, reproduction, and mortality), to infer the evolution of the population over time (Figure 1). In this section, we describe in more detail the different modules, parameters, and processes considered.

Environmental forcing

The environmental forcing was provided by the regional coupled physical–biogeochemical POLCOMS–ERSEM model (Holt *et al.*, 2001; Butenschön *et al.*, 2016), using a 0.1° spatial resolution and 40 sigma layers over the period 1996–2015. The model was forced using re-analysis for the atmospheric interface (ERAinterim, Dee *et al.* 2011) and physical ocean boundary conditions (GLORYS2v4, product GLOBAL_REANALYSIS_PHY_001_025 from marine.copernicus.eu), with the biogeochemical boundary conditions and river inputs set using climatology (World Ocean Atlas, www.nodc.noaa.gov/OC5/woa13/), GLODAPv2 (https://www.nodc.noaa.gov/ocads/oceans/GLODAPv2/), and GlobalNEWS2 (Mayorga *et al.*, 2010). Temperature (°C) and zooplankton biomass (mg C m^{-3}) outputs of this model were used to force the DEB–IBM model. Our model is not spatially explicit, so the forcing variables were averaged over the Bay of Biscay region from the coast to 48.0°N and 5.0°W (Figure 2 and Supplementary Figures S1–S4), which covers the distribution of the population over its life cycle. The depth considered for the temperature series was integrated between 0 and 150 m for adults and between 0 and 30 m for eggs, larvae, and juveniles (Gatti *et al.*, 2017), while the concentration of zooplankton in the first 50 m was used for the food density (Plounevez and Champalbert, 1999). Zooplankton biomass (X, mg C m^{-3}) was then introduced as food concentration in the DEB model, being used to calculate the "scaled functional response" for food (f) as a Holling type II function $f = X/(\underline{X} + K_f)$ (where K_f is the half-saturation coefficient for food, see Supplementary Table S1).

Individual bioenergetics modelling

The anchovy life cycle was described by means of a bioenergetic model based on the DEB theory of Kooijman (2010; DEB module). The values of the different parameters considered in this

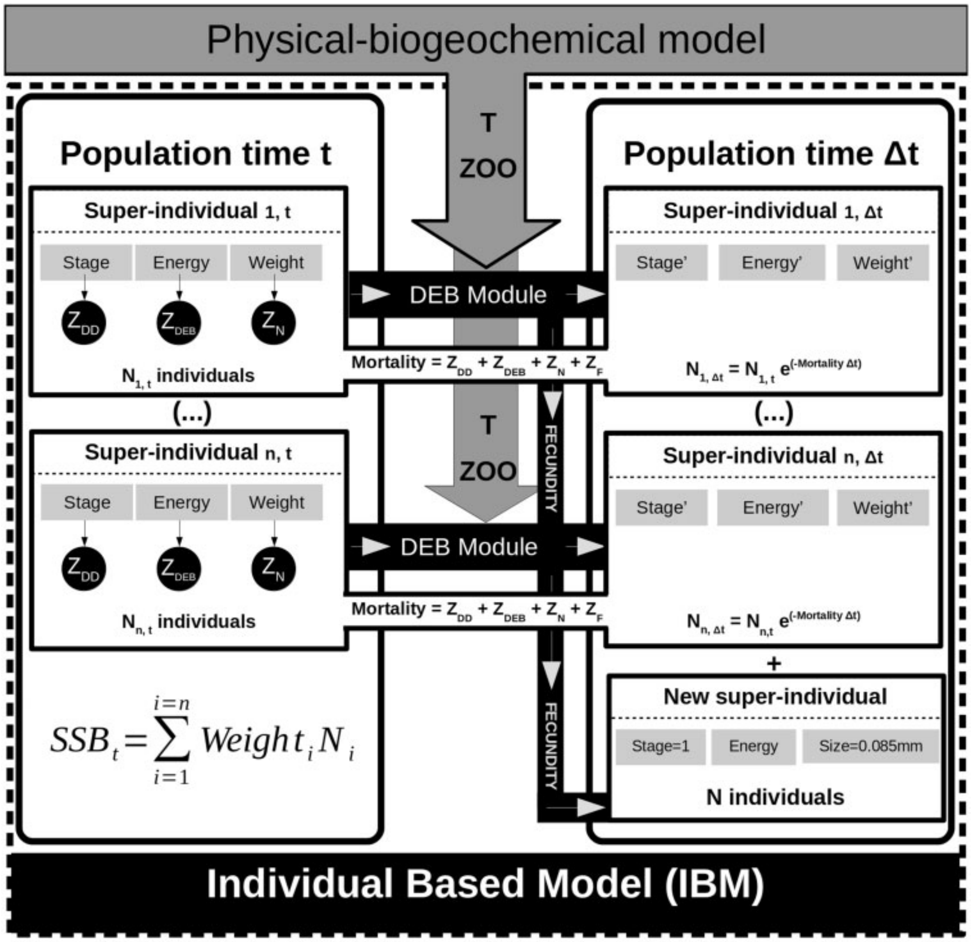

Figure 1. Schematic showing the integration of the population (IBM) and individual (DEB) modules over two consecutive time steps (t and Δt). We consider n SIs per time step, with n varying each Δt due to mortality (z) and fecundity. Temperature (T) and zooplankton concentration (ZOO) are provided by a regional physical–biogeochemical model that forces the bioenergetics of each SI (DEB module), making them change over time. Reproduction events can occur every 3 d between April and September. An SI disappears when all its individuals are dead. For each reproductive event, a new SI is created, being the sum of all the eggs spawned by the whole set of individuals of the population its initial number of individuals. Mortality sources correspond to Z_{DEB}: energetic failure (inability to allocate the required energy to maintenance); Z_N: natural mortality [related to body size, which is calculated from body weight, as described in Equation (1)]; Z_F: fishing mortality (obtained from the literature, constant value per semester); Z_{DD}: density-dependent larval mortality [only applied to the larval stage and dependent on the estimated concentration of eggs, as described by Somarakis and Nikolioudakis (2007), see Equation (2)].

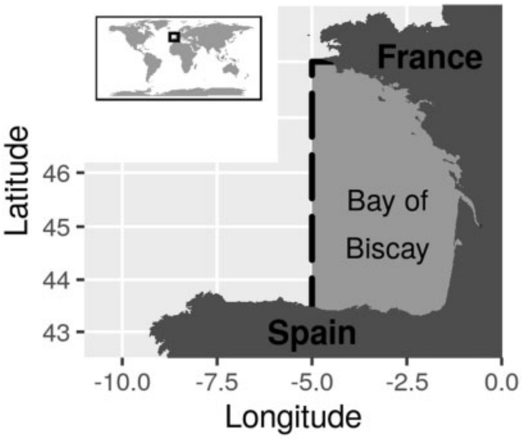

Figure 2. Location of the Bay of Biscay and the geographical extent considered in the analysis (grey area).

model are shown in Supplementary Table S1, while the equations describing the main processes of the individual metabolism are presented in Supplementary Table S2. Forcing the DEB module with a physical–biogeochemical model for the Bay of Biscay (Figure 2) makes it possible to evaluate the impact of environmental variables on metabolic-dependent processes at the individual level such as growth, fecundity, or mortality.

The DEB module used here was calibrated for the Bay of Biscay anchovy by Gatti *et al.* (2017). A simulation at the individual level using a daily environmental climatology of temperature and zooplankton from the period 1996–2015 ("individual run," Supplementary Figure S5), gave similar results to those of Gatti *et al.* (2017). However, because the coupled physical–biogeochemical model used as forcing was not the same than in their study, some minor adjustments to the maximum assimilation rate ($p_{\mathring{A}m}$) and the fraction of energy allocated to growth (k) were made (from 800 to 820 J cm^{-2} d^{-1}, and from 0.71 to 0.80, respectively).

Population modelling

The DEB module was coupled to an IBM. Superindividuals (SIs) were used as modelling units (Scheffer *et al.*, 1995; Rose *et al.*, 2015), in which each SI represented a large number of individuals born the same day and with identical life history and parameters. We integrated overall SIs to scale-up the response to environmental factors at the population level (IBM module). This consisted of the addition of the processes and state variables of the individuals forming each SI across the population (i.e. fecundity, biomass, growth, mortality, etc.), to infer the characteristics of the whole population. The population was initialized on 1 April 1996 and the model was run until 31 December 2015, with years 1996–1999 used as a "spin-up" period to stabilize the population in terms of SI number. The initial number of individuals within each parental SI was derived from the age-structured data obtained in PELGAS surveys (Doray *et al.*, 2018), while their size (g) and energy content on each of the DEB compartments (structural, reserve, and reproductive) were obtained from the individual run (Supplementary Figure S5). On the basis of this, the model started on 1 April 1996 with four adult SIs comprising different numbers of individuals (3.7×10^9, 1.5×10^9, 3.6×10^8, 2.4×10^7), with different age (1, 2, 3, 4 years), size (12.13, 16.20, 17.21, 17.56 cm), and energy in the different compartments of the DEB models: structure (20 625, 45 958, 50 914, 58 395 J), and reserve buffer (7548, 20 676, 26 693, 34 644 J). The energy of the reproductive buffer was the same for each initial SI: 12 026 J. The SIs were allowed to spawn every 3 d between April and September, creating new generations of SI during the "spin-up" period. All eggs spawned within 3 d by all adult SI were gathered in a unique new SI. The population variability in the model is generated by the effect of the different environmental variables experienced by SIs born at different moments of the year. In this manner, a pool of life histories during the spin-up period was originated, giving rise to a diversified population of 130 SIs on 1 January 2000, when the calibration period started (see below). The frequency for creating new SIs, which in turn controls the number of SIs in the model, was subject to a sensitivity analysis prior to the simulations. The objective was to find the lowest number of SIs which allowed faster simulations without effects on the model results, i.e. allowing enough variability to be simulated based on the different life-history trajectories of each SI.

Four sources of mortality were considered within the DEB–IBM framework. These mortalities are dependent on the energetic requirements, size, and stage of the fish, while the fishing mortality is considered as an external (fixed by semester) source of mortality. The mortality by energetic deprivation (Z_{DEB}) is explicitly included in the DEB module. It occurs when a fish cannot supply the required energy for somatic maintenance costs, neither from its reserve nor from emergency maintenance processes (reallocation from reproduction). This kind of mortality essentially occurs in late winter within our model in the Bay of Biscay.

Second, the natural mortality (Z_N) considers implicitly the effects of predation and decreases with individual size (Supplementary Figure S6):

$$Z_N = Z_a + (Z_e - Z_a)\mathrm{e}^{-z(L_T - L_{\mathrm{egg}})}, \tag{1}$$

with Z_a and Z_e the instantaneous mortality rate of adults and eggs, respectively, and z a decreasing coefficient of natural mortality. L_T is the individual length at a given time and L_{egg} is the average size of an anchovy egg in the Bay of Biscay (0.0854 cm, Huret *et al.*, 2016). These parameters (Z_a, Z_e, and z) are optimized during the calibration process (see below).

The third source of mortality is a density-dependent relationship between egg concentration and larval mortality established following the relationship by Somarakis and Nikolioudakis (2007) set in the Aegean Sea (Supplementary Figure S6):

$$Z_{\mathrm{DD}} = -0.154 + s\,\log(A), \tag{2}$$

with Z_{DD} the larval density-dependent mortality (applied until individual size = 2.81 cm, Supplementary Figure S6) and A the concentration of eggs, expressed in number m^{-2} (we considered 50 000 km^2, more or less half of the area of study, representing the potential spawning area of anchovy). The value of the slope [$s = 0.205$, according to Somarakis and Nikolioudakis (2007)] was also optimized during the calibration process (see below).

Finally, the fishing mortality (Z_F, Supplementary Figure S6) was introduced as a constrained external parameter with an updated value for every semester between 2000 and 2015 (data from ICES, 2018). Fishing mortality is considered as:

$$N_{t+\Delta t} = N_t e^{(-Z_F \Delta t)}, \tag{3}$$

where N_t and $N_{t+\Delta t}$ are the fish abundances at time t and $t+\Delta t$, respectively, being Δt the length of time step (1 h). This mortality rate was applied to adults and juveniles (not yet matured) during the first semester of the year and to actively reproducing adult individuals during the second semester of the year.

Model calibration with optimization of mortality parameters

The outputs from a Bayesian two-stage biomass-based model (CBBM, Ibaibarriaga *et al.*, 2008) were considered as reference for anchovy biomass in the Bay of Biscay between 2000 and 2015. These estimations are provided for 1 January. CBBM is the standard population assessment provided by ICES and considers two kinds of individuals in the population: adults participating in reproduction (spawning stock biomass, SSB) and recruits (age 1 adults that do not participate in reproduction). The biomass values were obtained from the model based on individual weight, the total number of individuals, and their age on 1 January. The differences between the outputs of the IBM model and the CBBM model were then computed as a cost function:

$$\sum_i \sum_y \left(\frac{B_{i,y} - B'_{i,y}}{\sigma_i} \right), \tag{4}$$

where $B_{i,y}$, and $B'_{i,y}$ are the simulated and observed (CBBM) biomass of class i (SSB and recruits), respectively, at time y (year), and σ_i is the standard deviation of $B'_{i,y}$. The cost function was calculated iteratively using a Nelder–Mead simplex optimization method (Nelder and Mead, 1965) considering different combinations of the following four parameters: the daily mortality rate of eggs [Z_e, Equation (1)], the mortality rate of adults [Z_a, Equation (1)], the coefficient of natural mortality scaling the decrease in mortality with size [z, Equation (1)], and the slope of the density-dependent relationship between egg concentration and larval mortality [s, Equation (2)]. The choice of these parameters for optimization was based on the difficulty of assessing mortality values in the field and the scarcity of the related literature.

As described above, our modelling approach allows to assess the impact of the mortality caused by winter starvation on the population (Z_{DEB}). This parameter is often disregarded in fish population modelling due to the empirical difficulties of estimation. By running a simulation where this source of mortality is disregarded, we were able to highlight its relevance for the population, which can be seen as an added value of our work. To make a simulation with no death by starvation—making sense when compared to the base-case simulation—it was necessary to consider a new calibration of the mortality parameters Z_a, Z_e, z, and s, in the same manner as described above.

Model validation

The model validation consisted of the comparison of the model outputs to independent data from scientific surveys for the stock assessment. Acoustic surveys for the stock assessment of anchovy in the Bay of Biscay are carried out during PELGAS spring surveys by the Institut Français de Recherche pour l'Exploitation de la Mer, IFREMER (France; Doray *et al.*, 2018). A second dataset comes from BIOMAN spring surveys conducted by AZTI-Tecnalia (Spain), which use the daily egg production method for an independent stock assessment of anchovy in the Bay of Biscay. In the validation of our model, both the number of individuals and their weight are taken into account to obtain the equivalent of the population SSB provided by the surveys. The outputs of our model were extracted in spring (15 May) for comparison with these surveys. In order to obtain a statistical measurement of the model validation, we estimated the significance of the slope (H_0: slope = 0) from the linear regression between the model and both independent time series (PELGAS and BIOMAN).

Hypotheses and scenarios

In order to study the separate effects of fishing mortality and environmental variables on population dynamics, different scenarios combining fishing pressure and environmental forcing were defined (Table 1). Scenarios were defined based on different hypotheses about the relationship between external forcing and population response. First, in order to show the effect of fishing, the inter-annual variability of the environment was disregarded and instead, a daily climatology of temperature and zooplankton computed over the period under study was used (scenario 1). Similarly, to study the effect of the environment on the population, fishing mortality (Z_F) was set constant (as the average of the whole time series) over the full period of study (scenario 2), or just during the fishing ban (scenario 3), aiming at understanding the effects of fishing over the entire period and the consequences of the fishing ban between 2005 and 2010.

Our modelling approach can also test the effect of different harvest rates or control rules on the stock performance. The current HCR has been implemented since 2010 (ICES, 2018) and is used to define a total allowable catch (TAC, in tonnes) of anchovy in a given year in the Bay of Biscay. This TAC, implemented from January to December of year $y+1$, is calculated based on the SSB at the end of the first semester of year $y+1$ as follows:

- $\mathrm{TAC}_{y+1} = 0\,\mathrm{t}$; if $\mathrm{SSB}_{y+1} \leq 24\,000\ \mathrm{t}$
- $\mathrm{TAC}_{y+1} = -2600 + 0.40 * \mathrm{SSB}_{y+1}$; if $24\ 000\,\mathrm{t} < \mathrm{SSB}_{y+1} \leq 89\ 000\ \mathrm{t}$
- $\mathrm{TAC}_{y+1} = 33\,000\ \mathrm{t}$; if $SSB_{y+1} > 89\,000\ t$

Table 1. Hypotheses on the influence of environment and fishing on the anchovy's population dynamics between 2000 and 2015, with scenarios proposed for testing them.

Hypothesis	Scenario
Hindcasted environmental variables and historical fishing mortality replicate the past dynamics of the population	(Sc0) Historical environmental forcing + historical fishing pressure
Fishing pressure drives population dynamics	(Sc1) Historical fishing pressure + average environmental forcing (as daily climatology) in the period 2000–2015
Environmental variables drive population dynamics	(Sc2) Historical environmental forcing + constant fishing pressure
The closure of the fishery was necessary for the recovery of the population	(Sc3) Historical environmental forcing + historical fishing pressure except between 2005 and 2010, when set constant
The implementation of the current HCR in the beginning of the time series would have prevented the collapse of the population	(Sc4) Historical environmental forcing + HCR fishing pressure

SSB_{y+1} is estimated by the assessment group on December of year y based on a recruitment prediction for year $y+1$. As we cannot make this projection in our model, we calculate the TAC based on the modelled SSB on 15 May of the current year and apply it from that date to the same date of the following year.

To include the HCR in the DEB–IBM model, it was necessary to translate it to an instantaneous mortality rate as Z_F. To do this, we extracted the SSB from our model on 15 May each year and the corresponding TAC was calculated according to the rules presented before. Then, using the average individual weight of adults and juveniles, we transformed the TAC into the number of individuals that can be captured (TAC′) during the season, obtaining the instantaneous fishing mortality (Z_F in year^{-1}) corresponding to the TAC′ as:

$$Z_F = -\ln\left(\frac{N_m - \mathrm{TAC}'}{N_m}\right), \tag{5}$$

where N_m is the number of individuals on 15 May in the population. To investigate if the application of the HCR would have avoided the collapse of the population, we defined a scenario where this strategy was applied since 2000 (scenario 4).

Results

Environmental variables

The environmental forcing variables used to run the model between 1996 and 2015 are shown in Supplementary Figures S1–S3. These figures also show the daily climatologies used for the calibration of the individual DEB and to run scenario 2, while in Supplementary Figure S4 a summary of four descriptors are shown for each year: annual mean temperature between 0 and 30 m, annual mean temperature between 0 and 150 m, annual mean zooplankton concentration, and the day of the year when the highest concentration of zooplankton occurs. Years 2003, 2014, and 2006 showed summer surface temperatures well over the daily 2000–2015 climatology (Supplementary Figures S1, S2, and S4). These years, except of 2006, presented also an earlier zooplankton bloom (Supplementary Figure S3), albeit the annual maximum could happen later in the year (Supplementary Figure S4). Year 2011 showed high spring temperature (Supplementary Figure S1), with an advanced zooplankton bloom (Supplementary Figures S3 and S4), but summer temperature was colder than the climatology. Years 2002, 2010, and 2013 were colder than the average in winter and spring, while no special feature was identified in zooplankton production during these years (Supplementary Figures S1–S4). No clear temporal patterns were found within the environmental forcing variables apart from an increasing mean zooplankton concentration (Supplementary Figure S4C, $p = 0.0535$).

Simulation at the individual level

The bioenergetic model captured successfully the dynamics of individual growth and energy density when using the daily 2000–2015 climatology as environmental forcing (Supplementary Figure S5, see also Gatti *et al.*, 2017). Individual growth in weight and length, and energy density of individuals (see Gatti *et al.*, 2017 for details on calculation) matched the observations from the surveys (dots in Supplementary Figure S5, see Gatti *et al.*, 2017 for data origin). According to these simulations, individual length and weight reached an asymptote at around 18 cm and 37 g, respectively. The model captured the variations in weight and energy density occurring on a seasonal scale based on the reproductive cycle and food availability.

Reconstruction of the past population dynamics

The DEB-IBM model was able to capture the main features of the population dynamics of the European anchovy between 2000 and 2015 in the Bay of Biscay (Figure 3a). This includes the collapse of the population in 2005 and the recovery afterwards. Four parameters were optimized (see Material and methods section): the daily adult mortality coefficient [Equation (1), $Z_a = 0.000001$], the daily egg mortality coefficient [Equation (1), $Z_e = 0.2494$], the coefficient parameterising length-decreasing natural mortality [Equation (1), $z = 0.3491$], and the slope of the density-dependent mortality of larvae [Equation (2), $s = 0.1418$]. Similarly to the CBBM values, the biomass predicted by our model (Figure 3a) decreased in the first few years of the simulation, with minimum values in 2005–2006 and two main drops in 2004 and 2007. After 2008, however, the population followed a steady and slow recovery until the end of the simulation, with a drop in 2014 (Figure 3a). The regression between the simulated and CBBM biomass values is significant ($r^2 = 0.40$; $p = 0.0039$).

The model was validated using biomass and weight-at-age values from biomass estimation surveys PELGAS and BIOMAN (see Material and methods). As on 1 January (Figure 3a), the population biomass on 15 May reached a minimum in 2005 and recovered afterwards (Figure 4a). A second important drop was also found in 2012. These dynamics are broadly coincident with the results from the research cruises, including the drop near the end of the time series (Figure 4a). The regression between observations and the model outputs showed significant relations ($p = 0.020$ PELGAS; $p = 0.0563$ BIOMAN), although the fit was poor ($r^2 = 0.327$ PELGAS; $r^2 = 0.236$ BIOMAN; Figure 4b). In addition, the weight-at-age on 15 May for the different ages in the population agreed with the survey data, albeit the inter-annual variability in the model outputs was lower (not shown).

From the DEB–IBM simulations, a variety of ecological indicators can be extracted to understand the mechanisms underlying the population dynamics (Figure 5). The age structure of the population in terms of number of individuals can be obtained at different times of the year. On 1 January, the proportion of age 1 individuals was found to be around 80% (Figure 5a), while on 15 May it decreased to around 50% (Figure 5b). DEB mortality, at the end of winter, is hence largely responsible for the loss of a high percentage of simulated age 1 individuals (Figure 6), 2014 being the year with the highest drop in the proportion of age 1 individuals between 1 January and 15 May (Figure 5b). This can be also appreciated in Supplementary Figure S7A and B, where the number of recruits on 1 January and 15 May is shown.

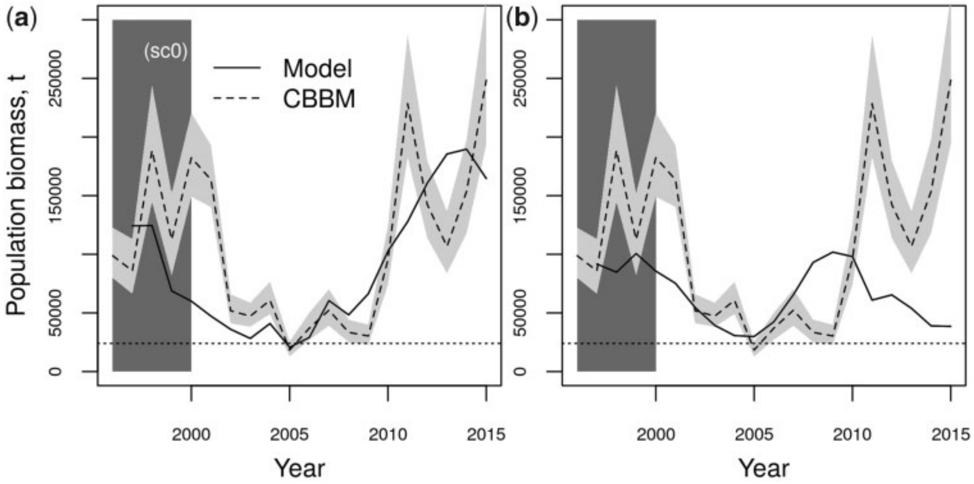

Figure 3. Model output (black solid line) for the biomass of anchovy in the Bay of Biscay on 1 January, considering the mortality by energetic failure within the DEB model (Z_{DEB}) [(a) scenario 0), and when this source of mortality is not considered (b). The dashed line represents the CBBM data with 95% confidence intervals (grey shadow). The dark background shows the spin-up period of the model (1996–1999), and the horizontal dotted line shows the 24 000 *t* limit stated by the HCR to close the fishery.

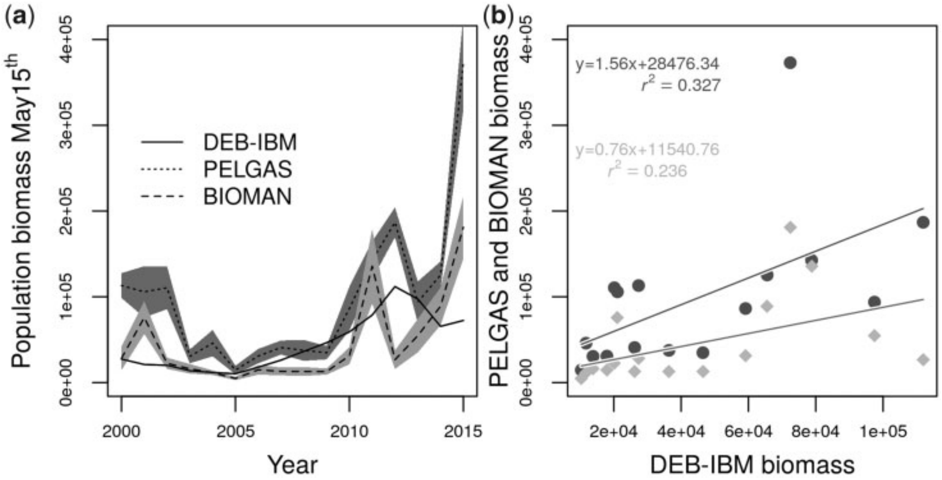

Figure 4. Model validation. (a) Time series of population biomass (tonnes) on 15 May, with reference values from PELGAS (pointed line) and BIOMAN (dashed line), with 95% confidence intervals shown for both reference estimates. (b) Linear regressions between model output and biomass reference values from PELGAS (dark grey) and BIOMAN (light grey).

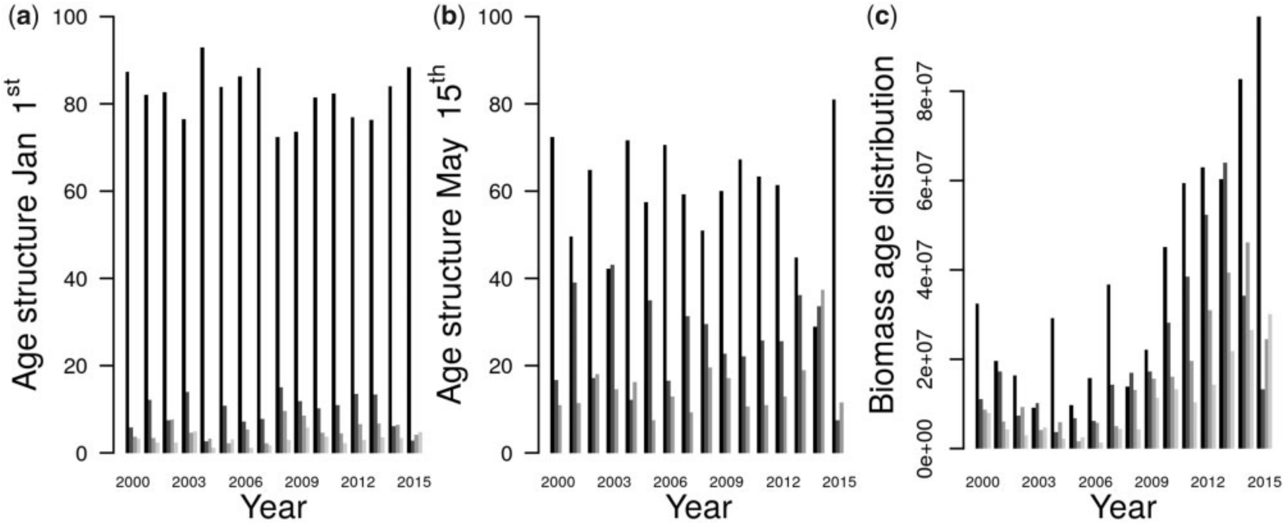

Figure 5. Ecological indicators obtained from the DEB–IBM model (I). (a) Proportion, in number of individuals, of each age class on 1 January. (b) Proportion, in number of individuals, of each age class on 15 May. (c) Biomass distribution (tonnes) by age class on 1 January. The colours of the bars represent the different age classes: age 1, age 2, age 3, and age 4 from black to light grey.

Similarly, the age structure in terms of biomass (Figure 5c, 1 January), shows that age 1 individuals are not so dominant as in terms of numbers of individuals and that the proportion corresponding to the different age classes did not vary significantly during the time series.

Different ecological indicators obtained from the DEB–IBM model show a drop in the performance of the population in 2004 (Supplementary Figure S7): egg survival, fertility, mean weight gain between January and May, Fulton's index as the condition factor, average adult weight, and the energy content of individuals in different DEB compartments. The energy density of age 1 individuals on 1 January did not show any special characteristic between 2004 and 2005, but dropped significantly in 2013 and 2014 (Supplementary Figure S7E). The average size at age did not vary significantly between 2000 and 2015 (Supplementary Figure S7H), with the highest interannual variation found for age 1.

The contribution of each source of mortality to the total mortality was estimated with the DEB–IBM model (Figure 6). The starvation mortality (Z_{DEB}) affected age 1 individuals only. It happens at the end of winter when the recruits have insufficient resources and therefore die. Fishing mortality (Z_F) was more important than natural mortality for ages 2, 3, and 4, affecting age 1 as well. Natural mortality (Z_N) decreases in importance as fishes grow (Supplementary Figure S6). Within the hindcasted period, Z_{DEB} was found to be especially high in 2004 and 2007. After 2008, Z_{DEB} dropped for age 1 individuals, until 2014 when it suffered a sudden increase.

The simulation where Z_{DEB} was not included in the DEB model (additional simulation, Figure 3b) required a different

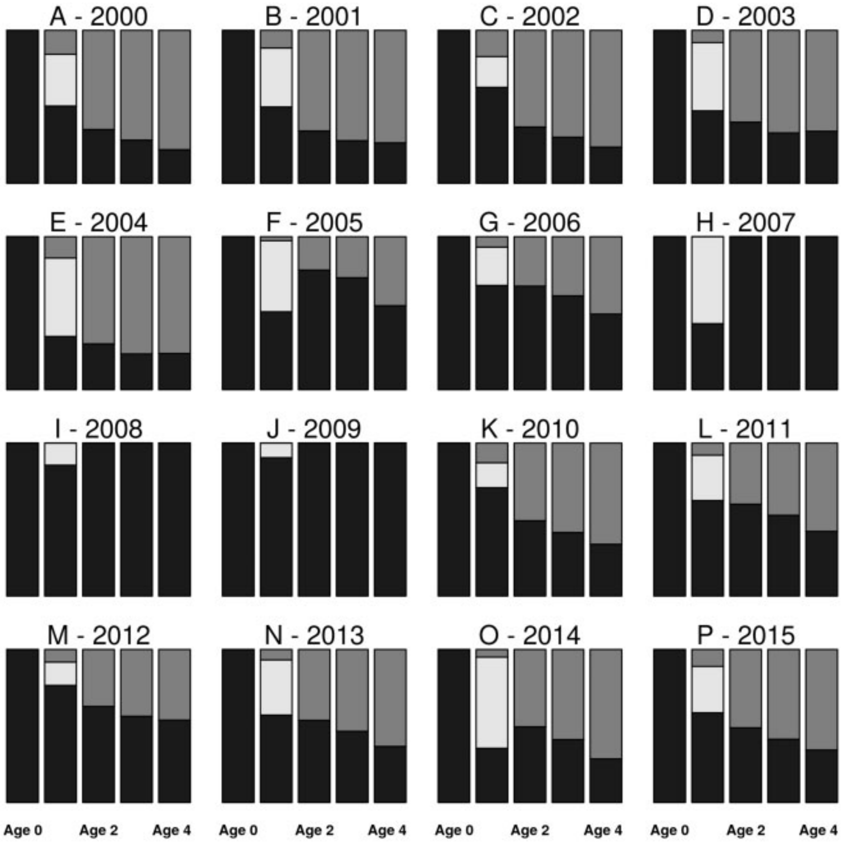

Figure 6. Ecological indicators obtained from the DEB–IBM model (II). Sources of mortality by age and year as a proportion of the total number of dead individuals of a given age and year during the simulation. Black: natural mortality; white: DEB mortality; grey: fishing mortality.

calibration of the mortality parameters ($Z_a = 0.0004$, $z = 1.045$, $Z_e = 0.950$, $s = 0.172$). In this simulation, the population was found to drop from the beginning of the period until 2005, recovering afterwards and dropping again by the end of the simulation (Figure 3b). Part of the inter-annual variability was lost, and many indicators were substantially different from scenario 0 (Supplementary Figure S8). The proportion of individuals dying by fishing mortality was increased, while the energetic minima of 2004, 2007, and 2014 were also captured under this simulation.

Fishing and climate scenarios

Following the scenarios approach shown in Table 1, applying a constant fishing mortality rate with the historical environmental forcing should demonstrate the real impact of environmental forcing alone (scenario 1; Figure 7a). In this simulation, the population dropped during the first years but to a lower extent than when the real fishing mortality was applied (Figure 3a and the grey line in Figure 7a). Then, the population reached two minima, in 2003 and 2005, dropping again in 2008. At the end of the simulation, the population did not increase as much as under scenario 0. The inter-annual variability was found to be higher in scenario 1 than in scenario 0 (Figure 7a). Supplementary Figure S9 shows the different ecological indicators extracted from this simulation. The age composition of the population was similar to scenario 0, while the recruitment was higher in the beginning of the time series but lower in the end. The drop of indicators found in 2004 under scenario 0 was also found for the weight gain between January and May, the Fulton's condition factor, the egg survival, and the fecundity. According to the energetics of individuals, important drops were also registered in 2004, 2007, and 2014.

In scenario 2 (fishing alone drives population dynamics: Table 1 and Figure 7b), the population was found to suffer a drastic increase after the closure of the fishery in 2005, stabilizing at the end. The inter-annual variability was found to be much lower than in scenarios 0 and 1, which is also evident in a range of ecological indicators (Supplementary Figure S10). The drop of performance found in scenarios 0 and 1 in 2004 was not so evident, but still present in this scenario, mainly referring to the Fulton's condition factor and the fecundity of individuals, while the survival of eggs decreased by the end of the simulation (Supplementary Figure S10G, I, and J).

Under scenario 3 (closure necessary for the recovery: Table 1 and Figure 7c), the population did not recover after the collapse of 2005, keeping minimal values until the end of the simulation. Ecological indicators showed the same patterns as in scenario 0 but with lower values by the end of the simulation. This is especially evident for the recruitment and for the proportion of age 1 individuals in terms of numbers and biomass (Supplementary Figure S11).

The simulation of the application of the current HCR from the beginning of the period (scenario 4) showed that the population did not drop at the beginning, being sustained well over the limit

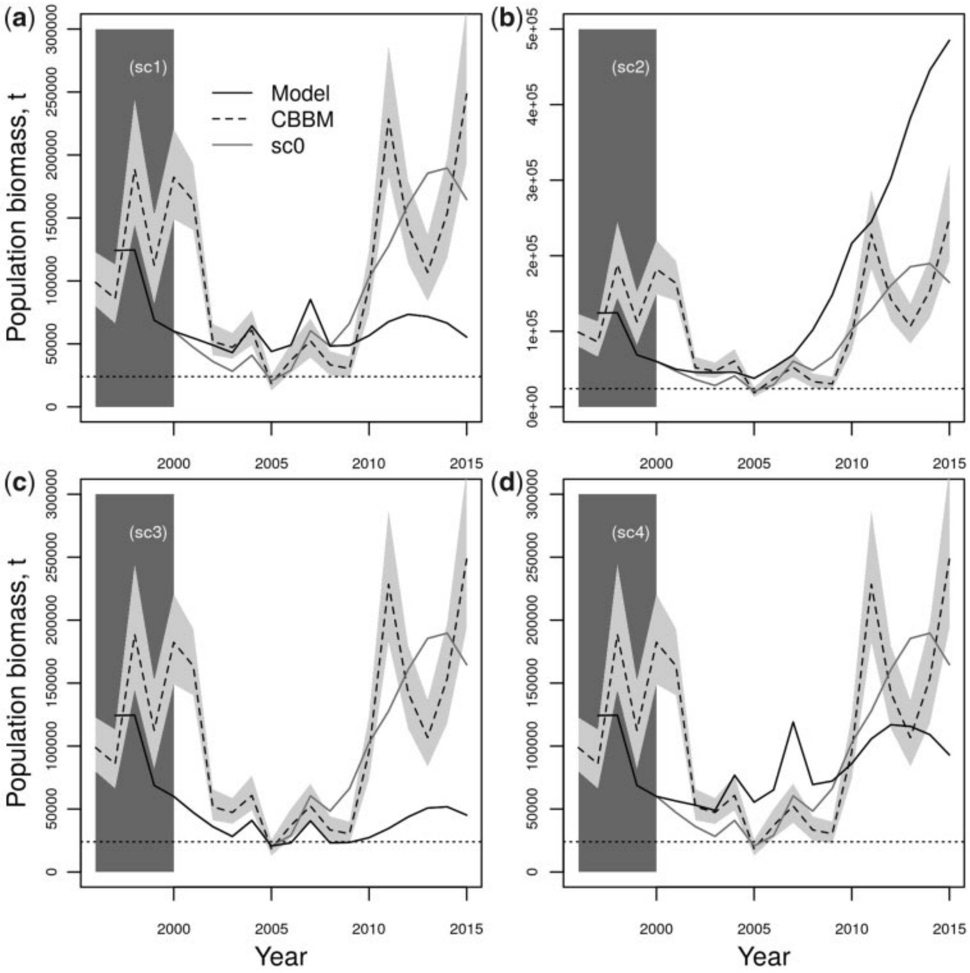

Figure 7. Model output (black solid line) for the biomass of anchovy in the Bay of Biscay on 1 January, using the different environmental and fishing scenarios described in Table 1: (a) constant fishing mortality at the average of the time series, with historical environmental forcing (scenario 1); (b) historical fishing mortality with constant environmental forcing as a daily climatology repeated year after year (scenario 2); (c) historical environmental forcing and fishing pressure, but assuming constant fishing mortality at the average of the time series between 2005 and 2010 (scenario 3); (d) implementation of the HCR since 2000 (scenario 4). The continuous grey line shows the population biomass from scenario 0 (Figure 3a) for comparison. The dashed line represents the CBBM data with 95% confidence intervals (grey shadow). The dark background shows the spin-up period of the model (1996–1999), and the horizontal dotted line shows the 24 000 *t* limit stated by the HCR to close the fishery.

of 24 000 tonnes established in the HCR to close the fishery (Figure 7d). The inter-annual variability was found to be coincident with scenarios 0, 1, and 3, while the final period, on the other hand, did not show the increase in population found in the scenario 0 simulation: instead, it was more or less stable around 100 000 tonnes. Ecological indicators also show similar patterns as those for scenario 1, with drops of individual performance in 2004, 2007, and 2014 and with lower recruitment values in 2003, 2005, 2008, and 2012 (Supplementary Figure S12).

Discussion

We integrated for the first time a bioenergetics model into a population model for the Bay of Biscay anchovy. This coupling framework successfully replicated the main patterns of the population dynamics between 2000 and 2015 (Figure 3a), including the initial drop, the collapse of 2005, and the recovery after 2008. In addition, by combining this approach with simulations based on different scenarios of environmental and fishing pressure, we provide new insights into the causes of the collapse of 2005 and on the recovery afterwards. Our results provide evidence that the inter-annual variability of the anchovy population was mostly driven by environmental conditions, while the effect of fishing was more evident on a longer-time scale. We also investigated the relevance of the closure of the fishery between 2005 and 2010 for the recovery of the population, as well as the likely consequences of the implementation of the current HCR before the collapse.

Including the effect of mortality associated with individual bioenergetics improved the hindcast ability of the model (Figure 4a vs b). The calibration considering Z_{DEB} (scenario 0; Figure 3a) provided estimates of egg (Z_e), and adult (Z_a) mortality rates consistently lower than values in the literature (Uriarte *et al.*, 2016). This result was expected as natural mortality measured in the literature should be comparable to the sum of Z_{DEB} and Z_N in our modelling framework. On the other hand, the values of Z_a and Z_e when Z_{DEB} was not taken into account (Figure 3b) were much higher. Furthermore, the inter-annual variability was better captured when Z_{DEB} was considered. This source of mortality could be very important for the recruitment success at the end of the first winter as it affects age 1 individuals. A negative (but non-significant) relationship between the number of recruits on 15 May and the proportion of dead individuals by Z_{DEB} in the previous winter (both estimated from our model) was found ($p = 0.091$; $r^2 = 0.19$). Hence, according to our results, this potential source of mortality establishes a direct link between the environmental variability and the resulting population dynamics. Due to inherent methodological difficulties, few references on natural mortality by starvation during winter for early stages of pelagic fish are available (but see Pepin, 2016a, b).

Population dynamics related to environmental and fishing

Simulating the anchovy population under different scenarios (Table 1) allowed us to study the effects of fishing and environment on the population dynamics. Hence, while scenario 1 (population subject to constant fishing mortality, Figure 7a) captured the inter-annual variability of the simulation of reference, it failed to replicate the drop and recovery of the population. On the other hand, under scenario 2 (no inter-annual variability of the environment, Figure 7b) the simulation did not capture the inter-annual variability of the population, but rather, the longer-term pattern of increase–decrease in biomass. These findings suggest a short-term control of the population by environmental drivers, while the effect of fishing would have effect on a longer-time scale. This is probably because of the autorecorrelation of the fishing pressure showing a clear temporal trend: high at the beginning of the simulation, minimal or null between 2005 and 2010, and intermediate between 2010 and 2015. In fact, the response of the population to the closure of the fishery under scenario 2 (constant environment) was immediate in 2005, demonstrating that fishing pressure could affect population dynamics in a short temporal scale as well.

Scenarios 1 (constant fishing) and 2 (constant environment) suggest a joint action of environmental and fishing on the drop and collapse of the population in the early 2000s. Hence, scenario 1 (and scenario 4, see below) showed that environment was unfavourable for the population during that period, and also, that a lower fishing mortality at the beginning of the time series would have prevented the collapse of the population (Figure 7a). On the other hand, the constant environment simulated in scenario 2 indicated that fishing pressure alone was sufficient to cause a low population before 2005, close to the 24 000 t limit established by the HCR to close the fishery (Figure 7b). The corollary of these simulations is that both factors contributed to the fall of the population, with the especially bad environmental conditions of 2004 being the definitive drivers of the collapse of the population in 2005 (see below a mechanistic discussion on the specific causes). This finding is in agreement with the work of Taboada and Anadón (2016), which showed that fishing pressure was fundamental to explaining the collapse of the population in 2005, in addition to environmental variables such as the phytoplankton bloom phenology or the larval drift.

In a similar manner, the recovery of the population after 2008 in our model was probably triggered by a combination of low fishing pressure and favourable environmental conditions. Figure 6 showed that the recovery period of the simulation had the lowest proportion of Z_{DEB} of the time series, while the simulation of scenario 4 (with no closure of the fishery; Figure 7d), demonstrated that the population would not have been able to recover if fishing had been kept constant between 2005 and 2010. Interestingly, as shown in the simulation of scenario 1 (constant fishing), the effect of lower Z_{DEB} would have not been sufficient to trigger the recovery of the population (Figure 7a), probably due to an increased fishing mortality in regards of scenario 0. In contrast, the closure of the fishery alone (scenario 2) would probably have been enough to allow the recovery of the population (Figure 7b) which, comparing with scenario 0, could have been faster than under variable environmental forcing. Hence, both the closure of the fishery and the drop of Z_{DEB} were beneficial and coincident in time for the population, finally triggering its recovery. The environmental causes of the drop of Z_{DEB} in this period are discussed below.

Mechanistic perspective of the population dynamics

The environmental features preceding the collapse of 2005 deserve special consideration to understand the mechanisms of action of environmental variables on the bioenergetics of individuals and populations. 2003 temperature was significantly high at both 0–30 and 0–150 m integrated depths (Supplementary Figures S1 and S2) with an early bloom of zooplankton in spring and low zooplankton concentration during the second part of the year (Supplementary Figure S3), while in 2004 temperature and zooplankton concentration were close to the average (Supplementary Figures S1–S3). As a consequence of the higher temperature, different indicators extracted from our model on 1 January 2004 indicate good individual performance during 2003: a higher proportion of the time series of age 1 individuals (Figure 5a), high proportion of age 1 individuals in terms of biomass (Figure 5c), high recruitment of individuals (Supplementary Figure S7A), age 1 individuals with high energy density (Supplementary Figure S7E), and large adults (Supplementary Figure S7I), with high energy levels (Supplementary Figure S7J). Conversely, indicators from the model obtained on 15 May 2004 show a trend change, with the lowest weight gain between January and May (Supplementary Figure S7C), and a critical drop of energetics between 2003 and 2004 (Supplementary Figure S7J). The drop of performance at the individual and population level is also in agreement with the high Z_{DEB} (Figure 6) shown by the model. This mortality is expected to take place at the end of winter when individuals cannot pay maintenance costs from food or from reserves.

The high and low performance of the modelled population in 2003 and 2004, respectively, can probably be explained from a bioenergetics perspective. The high temperature in 2003 contributed positively to the growth and reproduction of individuals in our model. Yet, despite many indicators showing good performance of the population at the beginning of 2004, the lower food during the second part of 2003 was the reason why age 1 individuals and adults showed low energy density in 2003 (Supplementary Figure S7E). This led to insufficient accumulation of reserves to face the winter and caused the drastic drop of energy observed between 2003 and 2004 (Supplementary Figure S7J). Furthermore, the high temperature of 2003 and the early zooplankton bloom could have favoured the growth of individuals in the first half of 2003, with a consequent increase of maintenance costs at the individual level (proportional to body volume). In this sense, the model predicts a trade-off along the size spectra, with lower predation-based mortality for bigger individuals but also higher risk to starve. This could make the population especially sensitive to subsequent 2003–2004 winter scarcity of food and explain the lowest in the time series weight gain as well as high bioenergetics mortality (Z_{DEB}) at age 1 between January and May 2004 (Supplementary Figure S7C). All these phenomena, together with the lowest fecundity of the time series in 2004 as a consequence of the low food in the second part of 2003 (Supplementary Figure S7G), led to the collapse of the population in 2005.

After 2005, several indicators showed positive trends for the recovery of the population. The proportion of individuals dying because of energetic failure (Z_{DEB}) in 2006 dropped and stayed low until 2012 (Figure 6), except for 2007. These years were warm in general (Supplementary Figures S1, S2, and S4), and with zooplankton in late autumn (Supplementary Figure S3), resulting in shortening of the winter period and thus decreasing starvation risk. In 2013, Z_{DEB} rose again, which coincided with a delay in the bloom of zooplankton resulting in food scarcity at the end of winter, increasing the mortality of age 1 individuals by starvation. This truncated the recovery of the modelled population between 2013 and 2014 according to our simulation. The observations from the CBBM, on the other hand, showed drastic drops of the biomass in 2011 and 2012. None of our simulations captured these features, but it is worth noting that CBBM estimates may be subject to considerable error as well.

Retrospective application of the HCR

One of the consequences of the closure of the fishery between 2005 and 2010 was the subsequent implementation of the HCR to estimate the TAC of anchovy in the Bay of Biscay. This measure established a lower SSB boundary of 24 000 tonnes to close the fishery and a maximal catch of 33 000 tonnes if the estimated SSB was higher than 89 000 tonnes (see Material and methods section and Sánchez *et al.*, 2019 for a deeper analysis of the HCR). Simulating this HCR from the beginning of the period is a direct application of the DEB–IBM approach and is useful for evaluating the utility of this policy to prevent the collapse of the population. Also, it permits us to analyse whether the upper TAC limit of 33 000 tonnes is sufficiently restrictive to avoid situations of risk for the population. In this manner, under scenario 4, we found that the biomass of the population remained well over the lower boundary of 24 000 tonnes during the whole simulation (Figure 7d), and also, that the biomass minimum occurred in 2003, after which the population started to increase slightly. This result shows that the current HCR could be adequate to avoid the collapse of the population under similar circumstances, but also showed that the population would have been impeded from growing as much as under scenario 0, where the closure of the fishery for 5 years was pivotal for the increase of the population to current values of around 150 000 tonnes (Figure 3a).

Model limitations and sensitivity analysis

The integrated DEB–IBM model presented here contains inherent noise related to model parametrization and estimated parameters. At the individual level, the genetic inter-individual variability within the population was not considered, instead the unique determinant of the individual life-history trajectory and phenotype was the environmental conditions from the birth date. Also, the model is constructed based on <20 parameters within the IBM and DEB modules that are subject to estimation errors (see Gatti *et al.*, 2017). These parameters were calibrated in regards of individual size, weight-at-age, seasonal data on energy density, and yearly time series of population biomass which further introduced some error. The overall error associated with the calibration of our mortality parameters is difficult to assess since the CBBM biomass time series used as reference is an estimation from an assessment model containing its own intrinsic uncertainties (Ibaibarriaga *et al.*, 2008). The density-dependent mortality (Z_{DD}), only applied to the larval stage in our model, likely affects juveniles and adults as well, introducing more error in the estimations of mortality. The initialization parameters used for the population in 1996 were also obtained from surveys (see Gatti *et al.*, 2017), being subject to estimation errors as commented before and introducing some noise into the model as well. Initialization parameters always influence simulations, and the purpose of this work was to use the most realistic set of initial conditions available from data. Hence, we considered the population structure and energetics, respectively, from the surveys (see Gatti *et al.*, 2017) and the individual run with climatological forcing (Supplementary Figure S5) as reliable data for initialization. Minor adjustments in DEB parameters ($p_{\mathrm{\mathring{A}m}}$ and K) relative to the work of Gatti *et al.* (2017) were applied in order to stabilize the population during the spin-up period. These parameters were chosen because they had the highest uncertainty of estimation. The stabilization of the population during the spin-up period was measured in terms of the number of SIs conforming the population (around 130), but still there was an important gap between the modelled population biomass and CBBM data in 2000.

At the population level, the model is not spatially explicit, which means that all the environmental variables are averaged over the area of study (Figure 1). This limits the effectiveness of the model because spatial processes, such as the variability in spatial distribution throughout the life cycle, or variability in larval drift, may explain part of the unresolved variability between the observations and the historical evolution of the population. In any case, it is also worth to mention that while new model components such as spatial detail, or individual variability, could increase the resolution of the model, they could also make predictions more uncertain if poorly parameterized. Furthermore, the outputs from the physical–biogeochemical model providing environmental data (POLCOMS–ERSEM) contain their own sources of error. Improving both aspects in our model (individual variability and spatial detail) seems to be necessary to increase the resolution of the model, whereas they could lead to more uncertain predictions if poorly parameterized.

Finally, a sensitivity analysis was carried out in order to determine the importance of variations of the considered environmental variables on the behaviour of the DEB–IBM model. This consisted of simulations of population biomass evolution under conditions of increased/decreased zooplankton concentration and temperature (Supplementary Figure S13). Generally, the response of the population was found to be favoured both by increased temperature and increased zooplankton, which could be understood from a bioenergetics perspective of metabolic enhancement leading to improved individual performance.

Conclusions

This is the first time that a bioenergetics model for the Bay of Biscay anchovy has been coupled to an IBM with the purpose of hindcasting the period of the population collapse and recovery at the beginning of the century. Our modelling approach allowed us to study the effect of the environmental and human pressures on the population of anchovy and showed that the environmental variability had immediate consequences on the population dynamics, while the effect of the fishery was apparent on a longer temporal scale. Moreover, the collapse of the population seems to have been a joint consequence of an elevated fishing pressure in the years preceding the collapse and unfavourable environmental conditions in the year before the collapse, with an exceptionally long winter (leading to food scarcity) causing a great natural mortality due to starvation. In the same manner, the recovery of the population was mainly triggered by the closure of the fishery for 5 years and favoured by warmer years with short winters leading to the appearance of larger individuals with high fecundity. Finally, a simulation of a retrospective implementation of the current HCR showed that this measure could have avoided the collapse of the population and the closure of the fishery in 2005.

Supplementary data

Supplementary material is available at the *ICESJMS* online version of the manuscript.

Funding

This work was funded by the Climate Change and European Aquatic Resources (CERES) project, which has received funding from the European Union's Horizon 2020 research and innovation programme under grant agreement no 678193.

References

Allain, G., Petitgas, P., and Lazure, P. 2001. The influence of meso-scale ocean processes on anchovy (*Engraulis encrasicolus*) recruitment in the Bay of Biscay estimated using a 3D hydrodynamic model. Fisheries Oceanography, 10: 151–163.

Allain, G., Petitgas, P., Lazure, P., and Grellier, P. 2007. Biophysical modelling of larval drift, growth and survival for the prediction of anchovy (*Engraulis encrasicolus*) recruitment in the Bay of Biscay (NE Atlantic). Fisheries Oceanography, 16: 489–505.

Borja, A., Fontán, A., Sáenz, J., and Valencia, V. 2008. Climate, oceanography, and recruitment: the case of the Bay of Biscay anchovy (*Engraulis encrasicolus*). Fisheries Oceanography, 17: 477–493.

Butenschön, M., Clark, J., Aldridge, J. N., Allen, J. I., Artioli, Y., Blackford, J. *et al.* 2016. ERSEM 15.06: a generic model for marine biogeochemistry and the ecosystem dynamics of the lower trophic levels. Geosciences Model Developments, 9: 1293–1339.

Checkley, D., Alheit, J., and Oozeki, Y. 2009. Synthesis and perspective. *In* Climate Change and Small Pelagic Fish, pp. 344–351. Ed. by J. Alheit and Y. Ooseki. Cambridge University Press, Cambridge, UK.

Cotano, U., Irigoien, X., Etxebeste, E., Álvarez, P., Zarauz, L., Mader, J., and Ferrer, L. 2008. Distribution, growth and survival of anchovy larvae (*Engraulis encrasicolus* L.) in relation to hydrodynamic and trophic environment in the Bay of Biscay. Journal of Plankton Research, 30: 467–481.

Cury, P., Bakun, A., Crawford, R. J. M., Jarre, A., Quiñones, R. A., Shannon, L. J., and Verheye, H. M. 2000. Small pelagics in upwelling systems: patterns of interaction and structural changes in "wasp-waist" ecosystems. ICES Journal of Marine Science, 57: 603–618.

Dee, D. P., Uppala, S. M., Simmons, A. J., Berrisford, P., Poli, P., Kobayashi, S., Andrae, U. *et al.* 2011. The ERA-Interim reanalysis: configuration and performance of the data assimilation system. Quarterly Journal of the Royal Meteorological Society, 137: 553–597.

Doray, M., Petitgas, P., Romagnan, J. B., Huret, M., Duhamel, E., Dupuy, C., Spitz, J. *et al.* 2018. The PELGAS survey: ship-based integrated monitoring of the Bay of Biscay pelagic ecosystem. Progress in Oceanography, 166: 15–29.

Fietcher, J., Rose, K. A., Curchitser, E. N., and Hedstrom, K. S. 2015. The role of environmental controls in determining sardine and anchovy population cycles in the California Current: analysis of an end-to-end model. Progress in Oceanography, 138: 381–398.

Gatti, P., Cominassi, L., Duhamel, E., Grellier, P., Le Delliou, H., Le Mestre, S., Petitgas, P. *et al.* 2018. Bioenergetic condition of anchovy and sardine in the Bay of Biscay and English Channel. Progress in Oceanography, 166: 129–138.

Gatti, P., Petitgas, P., and Huret, M. 2017. Comparing biological traits of anchovy and sardine in the Bay of Biscay: a modelling approach with the Dynamic Energy Budget. Ecological Modelling, 348: 93–109.

Holt, J. T., James, I. D., and Jones, J. E. 2001. An s coordinate density evolving model of the northwest European continental shelf 1, Model description and density structure. Journal of Geophysical Research, 105: 14015–14034.

Huret, M., Bourriau, P., Gatti, P., Dumas, F., and Petitgas, P. 2016. Size, permeability and buoyancy of anchovy (*Engraulis encrasicolus*) and sardine (*Sardina pilchardus*) eggs in relation to their physical environment in the Bay of Biscay. Fisheries Oceanography, 25: 582–597.

Huret, M., Tsiaras, K., Daewel, U., Skogen, M. D., Gatti, P., Petitgas, P., and Somarakis, S. 2019. Variation in life-history traits of European anchovy along a latitudinal gradient: a bioenergetics modelling approach. Marine Ecology Progress Series, 617–618: 95–112.

Huse, G., Giske, J., and Salvanes, A. G. V. 2002. Individual-based models. *In* Handbook of Fish Biology and Fisheries, pp. 228–248. Ed. by P. J. B. Hart and J. D. Reynolds. Blackwell Science Ltd, Oxford, UK.

Ibaibarriaga, L., Fernández, C., Uriarte, A., and Roel, B. A. 2008. A two-stage biomass dynamic model for Bay of Biscay anchovy: a Bayesian approach. ICES Journal of Marine Science, 65: 191–205.

ICES. 2018. Report of the Working Group on Southern Horse Mackerel, Anchovy and Sardine (WGHANSA), 26–30 June 2018, Lisbon, Portugal. ICES CM 2018/ACOM: 17. 607 pp.

Irigoien, X., Fernandes, J. A., Grosjean, P., Denis, K., Albaina, A., and Santos, M. 2009. Spring zooplankton distribution in the Bay of Biscay from 1998 to 2006 in relation with anchovy recruitment. Journal of Plankton Research, 31: 1–17.

Jakobsen, T., Fogarty, M. J., and Megrey, B. A. 2009. Fish Reproductive Biology: Implications for Assessment and Management. Wiley, New Jersey, USA.

Kooijman, S. 2010. Dynamic Energy Budget Theory for Metabolic Organisation, 3rd edn. Cambridge University Press, Cambridge, UK.

Letcher, B. H., Rice, J. A., Crowder, L. B., and Rose, K. A. 1996. Variability in survival of larval fish: disentangling components with generalized individual-based model. Canadian Journal of Fisheries and Aquaculture Science, 53: 787–801.

Mayorga, E., Seitzinger, S. P., Harrison, J. A., Dumont, E., Beusen, A. H. W., Bouwman, A. F., Fekete, B. M. *et al.* 2010. Global Nutrient Export from WaterSheds 2 (NEWS 2): model development and implementation. Environmental Modelling and Software, 25: 837–853.

Motos, L. 1996. Reproductive biology and fecundity of the Bay of Biscay anchovy population (*Engraulis encrasicolus* L.). Scientia Marina, 60: 195–207.

Nelder, J. A., and Mead, R. 1965. A simplex method for function minimization. Computer Journal, 7: 308–313.

Palomera, I., Olivar, M. P., Salat, J., Sabatés, A., Coll, M., García, A., and Morales-Nin, B. 2007. Small pelagic fish in the NW

Mediterranean Sea: an ecological review. Progress in Oceanography, 74: 377–396.

Pepin, P. 2016a. Reconsidering the impossible-linking environmental drivers to growth, mortality, and recruitment of fish. Canadian Journal of Fisheries and Aquatic Sciences, 73: 205–215.

Pepin, P. 2016b. Death from near and far: alternate perspectives on size-dependent mortality in larval fish. ICES Journal of Marine Science, 73: 196–203.

Pethybridge, H., Roos, D., Loizeau, V., Pecquerie, L., and Bacher, C. 2013. Responses of European anchovy vital rates and population growth to environmental fluctuations: and individual-based modelling approach. Ecological Modelling, 250: 370–383.

Plounevez, S., and Champalbert, G. 1999. Feeding behaviour and trophic environment of *Engraulis encrasicolus* (L.) in the Bay of Biscay. Estuarine, Coastal and Shelf Science, 49: 177–191.

Politikos, D. V., Curchitser, E. N., Rose, K. A., Checkley, Jr, D. M. , and Fiechter, J. 2018. Climate variability and sardine recruitment in the California Current: a mechanistic analysis of an ecosystem model. Fisheries Oceanography, 27: 602–622.

Politikos, D. V., Huret, M., and Petitgas, P. 2015a. A coupled movement and bioenergetics model to explore the spawning migration of anchovy in the Bay of Biscay. Ecological Modelling, 313: 212–222.

Politikos, D. V., Somarakis, S., Tsiaras, K. P., Giannoulaki, M., Petihakis, G., Machias, A., and Triantafyllou, G. 2015b. Simulating anchovy's full life cycle in the northern Aegean Sea (eastern Mediterranean): a coupled hydro-biogeochemical-IBM model. Progress in Oceanography, 138: 399–416.

Rose, K. A., Cowan, Jr, J. H. , Clark, M. E., Houde, E. D., and Wang, S.-B. 1999. An individual-based model of bay anchovy population dynamics in the mesohaline region of Chesapeake Bay. Marine Ecology Progress Series, 185: 113–132.

Rose, K. A., Fiechter, J., Curchitser, E. N., Hedstrom, K., Bernal, M., Creekmore, S., Haynie, A. *et al.* 2015. Demonstration of a fully coupled end-to-end model for small pelagic fish using sardine and anchovy in the California Current. Progress in Oceanography Part B, 138: 348–380.

Sánchez, S., Ibaibarriaga, L., Uriarte, A., Prellezo, R., Andrés, M., Abaunza, P., Jardim, E. *et al.* 2019. Challenges of management strategy evaluation for small pelagic fish: the Bay of Biscay anchovy case study. Marine Ecology Progress Series, 617–618: 245–263.

Scheffer, M., Baveco, J., DeAngelis, D., Rose, K., and van Nes, E. 1995. Super-individuals: a simple solution for modelling large populations on an individual basis. Ecological Modelling, 80: 161–170.

Somarakis, S., and Nikolioudakis, N. 2007. Oceanographic habitat, growth and mortality of larval anchovy (*Engraulis encrasicolus*) in the northern Aegean Sea (eastern Mediterranean). Marine Biology, 152: 1143–1158.

Somarakis, S., Palomera, I., García, A., Quintanilla, L., Koutsikopoulos, C., Uriarte, A., and Motos, L. 2004. Daily egg production of anchovy in European waters. ICES Journal of Marine Science, 61: 944–958.

Taboada, F. G., and Anadón, R. 2016. Determining the causes behind the collapse of a small pelagic fishery using Bayesian population modelling. Ecological Applications, 26: 886–898.

Uriarte, A., Ibaibarriaga, L., Pawlowski, L., Masse, J., Petitgas, P., Santos, M., and Skagen, D. 2016. Assessing natural mortality of Bay of Biscay anchovy from survey population and biomass estimates. Canadian Journal of Fisheries and Aquatic Sciences, 73: 216–234.

Vermard, Y., Marchal, P., Mahévas, S., and Thébaud, O. 2008. A dynamic model of the Bay of Biscay pelagic fleet simulating fishing trip choice: the response to the closure of the European anchovy (*Engraulis encrasicolus*) fishery in 2005. Canadian Journal of Fisheries and Aquatic Sciences, 65: 2444–2453.

Handling editor: Manuel Hidalgo